Biochemistry

 Volume 26, Number 2 January 27, 1987

Accelerated Publications

Proton Nuclear Magnetic Resonance Study of Hirudin: Resonance Assignment and Secondary Structure†

Dinesh K. Sukumaran, G. Marius Clore,* Axel Preuss, Jutta Zarbock, and Angela M. Gronenborn*

Max-Planck-Institut für Biochemie, D-8033 Martinsried bei München, FRG

Received October 7, 1986; Revised Manuscript Received November 7, 1986

ABSTRACT: The ^{1}H NMR spectrum of the 65-residue protein hirudin is assigned in a sequential manner by using a combination of two-dimensional nuclear magnetic resonance techniques to demonstrate through-bond and through-space (<5-Å) connectivities. The secondary structure of hirudin is deduced from a qualitative interpretation of the nuclear Overhauser effects involving the backbone NH, $C^{\alpha}H$, and $C^{\beta}H$ protons. It is shown that hirudin has two β-sheets and no α-helices.

Hirudin, a small protein of 65 residues from the leech *Hirudo medicinalis*, is the most potent natural inhibitor of coagulation known (Haycraft, 1884; Markwardt, 1970). Hirudin acts by binding specifically and very tightly ($K_{assoc} \sim 2 \times 10^{10}$ M^{-1}) to α-thrombin, thereby inactivating it and abolishing its ability to cleave fibrinogen (Magnusson, 1972; Markwardt, 1985; Stone & Hofsteenge, 1986). These remarkable properties have generated considerable interest with regard to the possible clinical use of hirudin as an antithrombotic agent (Nowak & Markwardt, 1980; Ishikawa et al., 1980; Walsmann & Markwardt, 1981; Markwardt et al., 1982; Kloss & Mittman, 1982).

In a series of recent papers the complete amino acid sequence of hirudin and the location of the three disulfide bridges have been determined (Badgy et al., 1976; Dodt et al., 1984, 1985, 1986). Further, the structural genes of two hirudin variants have been cloned into expression vectors and successfully expressed in *Escherichia coli* (Harvey et al., 1986; Bergmann et al., 1986). At the present time, however, nothing is known about either the secondary or tertiary structure of hirudin. Moreover, hirudin itself fails to crystallize, and the crystals of the thrombin–hirudin complex that have been obtained were unsuitable for X-ray crystallographic studies (W. Bode and R. Huber, personal communication). An alternative approach to solving the three-dimensional structure of hirudin is therefore called for. This involves the application of NMR[1] spectroscopy in solution (Wüthrich et al., 1982) and, in particular, the use of the nuclear Overhauser effect (NOE; Noggle & Schirmer, 1971) to obtain a large set of approximate interproton distances that can then be used as the basis of a three-dimensional structure determination using either distance geometry algorithms (Havel & Wüthrich, 1985; Braun & Go, 1985) and/or restrained molecular dynamics (Clore et al., 1985, 1986a,b; Kaptein et al., 1985; Brünger et al., 1986).

In this paper, we present the first step toward this goal, namely, the assignment of the ^{1}H NMR spectrum of hirudin using a combination of two-dimensional NMR techniques and the delineation of its secondary structure from a qualitative interpretation of the NOE data.

Experimental Procedures

Hirudin (batch CH.B.H3/5-720) was obtained from Plantorgan Werk (Bad Zwischenahn, FRG) as a gift from Dr. R. Maschler and Prof. E. Fink (Plantorgan) and Dr. D. Tripier (Hoechst) and was isolated and purified from the whole body of leeches as described previously (Bagdy et al., 1976). Purity was ascertained by sodium dodecyl sulfate–polyacrylamide gel electrophoresis, N-terminal residue analysis, amino acid analysis, and high-pressure liquid chromatography (D. Tripier, personal communication). The preparation contained one major species comprising 85% of the total and several minor

† This work was supported by the Max-Planck Gesellschaft (G.M.C. and A.M.G.).

[1] Abbreviations: NMR, nuclear magnetic resonance; NOE, nuclear Overhauser effect; NOESY, two-dimensional NOE spectroscopy; HOHAHA, homonuclear Hartmann–Hahn spectroscopy; DQF-COSY, double quantum filtered homonuclear correlated spectroscopy.

0006-2960/87/0426-0333$01.50/0

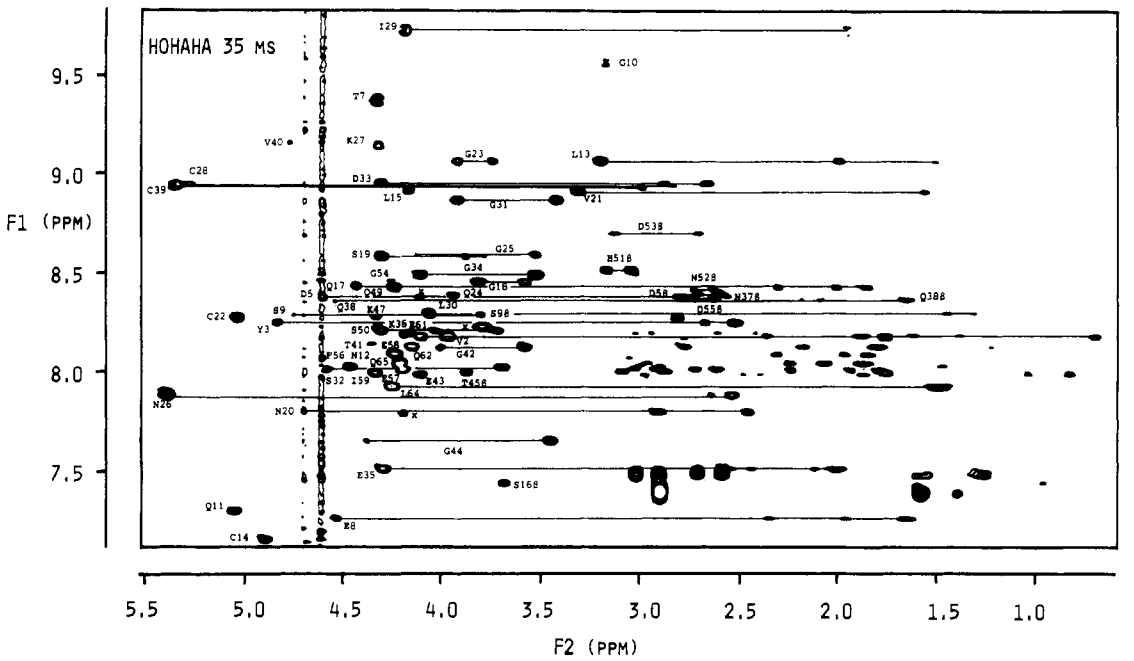

FIGURE 1: NH(F1-axis)–aliphatic(F2-axis) region of the HOHAHA spectrum of hirudin in H_2O. Some relayed connectivities are indicated by continuous lines, and the labels are at the positions of the direct NH–$C^{\alpha}H$ cross peaks except where indicated. The spectrum is unsymmetrized. Note that, in a few cases involving $C^{\alpha}H$ protons located directly under the water resonance such that the NH–$C^{\alpha}H$ cross peaks are no longer observable, the corresponding relayed cross peaks to the $C^{\beta}H$ protons are still apparent (e.g., N37, T5, D52, and D55). In this portion of the spectrum the NH–$C^{\alpha}H$ cross peaks of T4 and C6 (8.92, 4.63 and 8.90, 4.59 ppm), which are located just to the high field of the water resonance, are not visible and no associated relayed peaks could be observed; these NH–$C^{\alpha}H$ cross peaks, however, could be detected in the symmetrically related region of the HOHAHA spectrum. The three peaks marked x do not arise from native hirudin. They probably arise from the population of minor hirudin variants present (see Experimental Procedures).

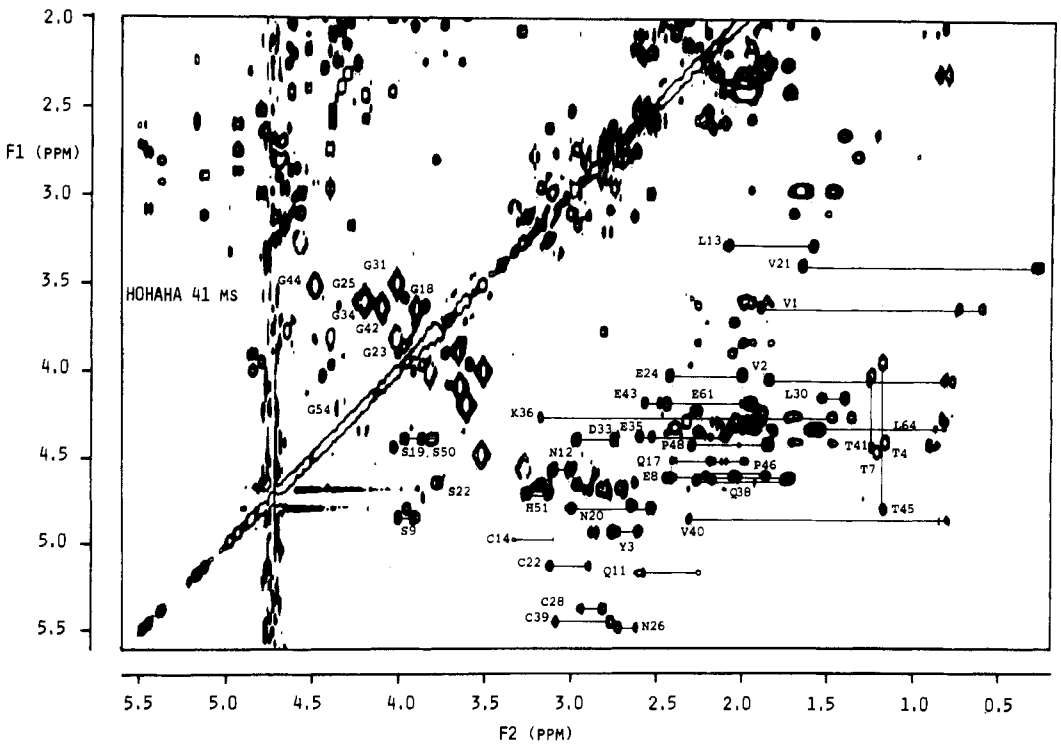

FIGURE 2: A portion of the $C^{\alpha}H$(F1-axis)–aliphatic(F2-axis) region of the HOHAHA spectrum of hirudin in D_2O. Direct and relayed connectivities are present, and some spin networks originating from the $C^{\alpha}H$ protons are indicated by continuous lines. The spectrum is unsymmetrized.

species comprising the remaining 15%. These minor species differ from the major one by single amino acid exchanges. Because each individual minor species comprises a very small percentage of the total, the resulting microheterogeneity posed no problems with respect to sequential resonance assignment. Samples for NMR contained 8 mM hirudin in either 90% H_2O/10% D_2O or 99.96% D_2O, pH 3.0.

NMR spectra were recorded on a Brüker AM500 spectrometer equipped with digital phase shifters and an ASPECT 3000 computer. All two-dimensional spectra were recorded in the pure phase absorption mode by using the time proportional incrementation method (Redfield & Kuntz, 1975) as described by Marion and Wüthrich (1983). The following spectra were recorded in D_2O and H_2O: NOESY (Jeener et

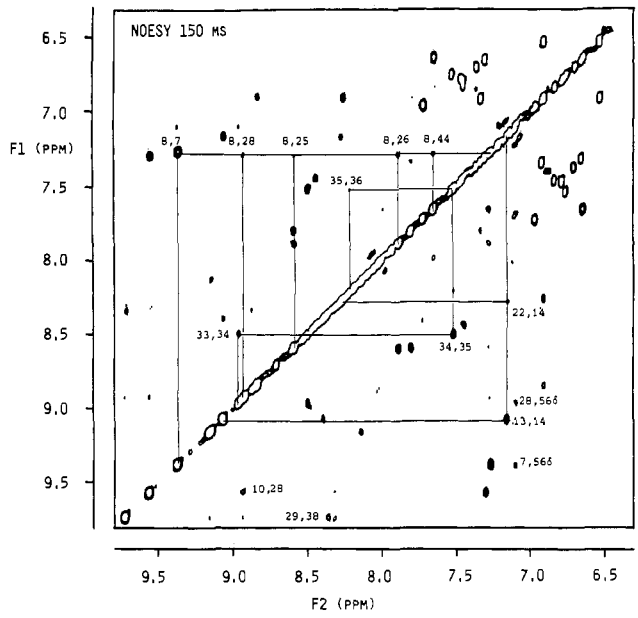

FIGURE 3: NH(F1-axis)–NH(F2-axis) region of the 150-ms NOESY spectrum of hirudin in H_2O. The sequence of $d_{NN}(i, i + 1)$ connectivities extending from residue 33 to residue 36 as well as that of some long-range d_{NN} connectivities is indicated. The spectrum is unsymmetrized and was recorded by using the semiselective jump–return sequence for the last 90° pulse to suppress the water resonance.

al., 1979) and MLEV17 HOHAHA (Bax & Davis, 1985). The HOHAHA spectra were recorded with mixing times ranging from 15 to 80 ms. The NOESY spectra were recorded at mixing times of 100, 150, 200, and 300 ms. For measurements in H_2O, the H_2O resonance was suppressed by irradiation during the relaxation delay and in the case of the NOESY spectra during the mixing time as well (Wider et al., 1984). An additional set of NOESY spectra in H_2O was also collected without solvent irradiation by replacing the last 90° pulse in the sequence by a semiselective jump–return (90_x–τ–90_{-x}) pulse with the carrier placed at the position of the water resonance (Plateau & Gueron, 1982). A digital resolution of 6.88 Hz/point in both dimensions was used for the NOESY and HOHAHA spectra. Typically 64–160 transients were recorded for each of 512 increments. A complete set of spectra was recorded at 25 °C. A NOESY spectrum (300-ms mixing time) in H_2O was also recorded at 5 °C. In addition, an ω_1-scaled (by a factor of 0.5) DQF-COSY spectrum (Rance et al., 1983; Brown, 1984) was recorded in H_2O at 25 °C with a digital resolution of 1.78 Hz/point in the t_2 dimension and 6.88 Hz/point in the t_1 dimension. All two-dimensional spectra were routinely processed for suppression of t_1 ridges by the method of Otting et al. (1986).

Results and Discussion

The essential prerequisite for the elucidation of a protein structure by NMR is the sequential assignment of resonances (Wüthrich et al., 1982). This was accomplished by identification of amino acid spin systems by means of direct and relayed through-bond connectivities, followed by sequential resonance assignment using short (<5-Å) through-space NOE connectivities involving the NH, $C^{\alpha}H$, and $C^{\beta}H$ protons as well as the $C^{\delta}H$ protons of proline (Wagner & Wüthrich, 1982; Zuiderweg et al., 1983; Strop et al., 1983; Kline & Wüthrich, 1985; Clore et al., 1985, 1986c; Wagner et al., 1986; Zarbock et al., 1986). Through-bond connectivities were identified by using HOHAHA spectra recorded at mixing times ranging from 15 to 80 ms in order to demonstrate successively direct, single-relayed, and multiple-relayed connectivities (Bax & Davis, 1985). Examples of HOHAHA spectra showing direct and relayed through-bond NH–aliphatic and $C^{\alpha}H$–aliphatic connectivities are shown in Figures 1 and 2, respectively. Through-space connectivities were identified by means of NOESY spectra recorded at mixing times ranging from 100 to 300 ms. Examples of NOESY spectra showing NH–NH,

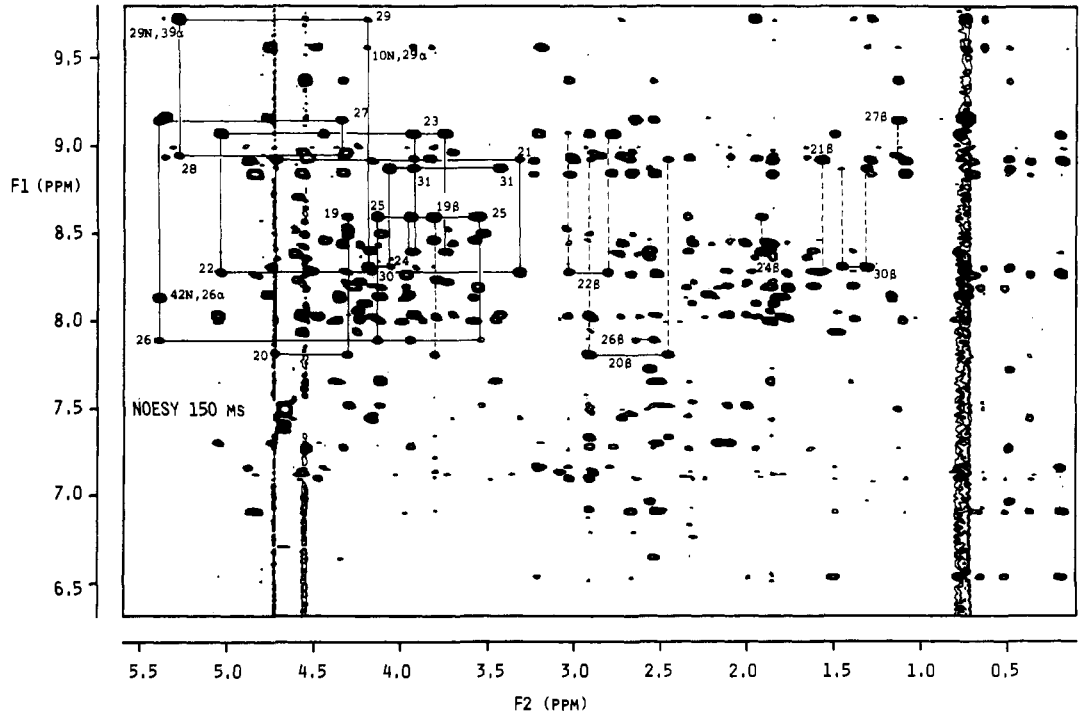

FIGURE 4: NH/aromatic(F1-axis)–aliphatic(F2-axis) region of the 150-ms NOESY spectrum of hirudin in H_2O. The sequence of $d_{\alpha N}(i, i + 1)$ connectivities extending from residue 19 to residue 31 is indicated by a continuous line, and the peaks are labeled at the positions of the intraresidue NH(i)–$C^{\alpha}H(i)$ cross peaks. Some $d_{\beta N}(i, i + 1)$ connectivities are indicated by dashed lines. Also labeled are a few long-range NH–$C^{\alpha}H$ connectivities. The spectrum is unsymmetrized and was recorded by using the semiselective jump–return sequence for the last 90° pulse to suppress the water resonance.

Table I: Protein Resonance Assignments of Hirudin at 25 °C and pH 3.0

residue	chemical shift (ppm) NH	$C^{\alpha}H$	$C^{\beta}H$	others	residue	chemical shift (ppm) NH	$C^{\alpha}H$	$C^{\beta}H$	others
V1		3.61	1.87	$C^{\gamma}H_3$ 0.70, 0.56	D33	9.03	4.37	2.94, 2.73	
V2	8.25	4.03	1.82	$C^{\gamma}H_3$ 0.74, 0.79	G34	8.56	4.17, 3.58		
Y3	8.32	4.90	2.73, 2.58	$C^{\delta}H$ 6.97; $C^{\epsilon}H$ 6.59	E35	7.58	4.36	2.16, 2.08	$C^{\gamma}H$ 2.58, 2.50
T4	8.91	4.63	4.39	$C^{\gamma}H_3$ 1.34	K36	8.26	4.24	1.69, 1.65	$C^{\gamma}H$ 1.44, 1.44; $C^{\delta}H$ 1.68, 1.59
D5	8.45	4.68	2.88, 2.88						$C^{\epsilon}H$ 3.15, 2.95; $N^{\zeta}H$ 7.55
C6	8.90	4.59	3.09, 2.60		N37	8.46	4.75	2.62, 2.62	NH_2 7.80, 7.04
T7	9.43	4.39	4.39	$C^{\gamma}H_3$ 1.18	Q38	8.41	4.61	1.89, 1.71	$C^{\gamma}H$ 2.25, 2.14
E8	7.34	4.60	2.01, 1.71	$C^{\gamma}H$ 2.49, 2.40	C39	8.99	5.42	3.06, 2.74	
S9	8.37	4.82	3.98, 3.88		V40	9.22	4.83	2.28	$C^{\gamma}H_3$ 0.83, 0.78
G10	9.62	4.54, 3.25			T41	8.22	4.42	4.03	$C^{\gamma}H_3$ 1.22
Q11	7.36	5.12	2.22, 2.18	$C^{\gamma}H$ 2.58, 2.55; NH_2 7.72, 6.71	G42	8.19	4.06, 3.64		
					E43	8.06	4.18	1.94, 1.94	$C^{\gamma}H$ 2.54, 2.46
N12	8.10	4.51	3.08, 2.98		G44	7.72	4.45, 3.52		
L13	9.13	3.26	2.06, 2.06	$C^{\gamma}H$ 1.56; $C^{\delta}H_3$ 0.85, 0.74	T45	8.05	4.76	3.94	$C^{\gamma}H_3$ 1.15
C14	7.23	4.95	3.10, 3.06		P46		4.58	2.18, 1.84	$C^{\gamma}H$ 2.03, 1.99; $C^{\delta}H$ 3.88, 3.70
L15	8.98	4.23	1.33, 1.13	$C^{\gamma}H$ 0.74; $C^{\delta}H_3$ 0.41, 0.13	K47	8.35	4.40	1.68, 1.64	$C^{\gamma}H$ 1.44, 1.44; $C^{\delta}H$ 1.68, 1.59
C16	7.51	4.69	3.77, 2.79						$C^{\epsilon}H$ 3.05, 2.95; $N^{\zeta}H$ 7.46
E17	8.51	4.50	2.08, 1.86	$C^{\gamma}H$ 2.38, 2.15	P48		4.41	2.27, 1.83	$C^{\gamma}H$ 1.99, 1.95; $C^{\delta}H$ 3.68, 3.57
G18	8.53	3.87, 3.63			Q49	8.50	4.32	2.05, 1.91	$C^{\gamma}H$ 2.37, 2.37
S19	8.65	4.36	3.95, 3.85		S50	8.28	4.39	3.79, 3.79	
N20	7.87	4.78	2.98, 2.51	NH_2 7.39, 6.98	H51	8.58	4.68	3.23, 3.10	$C^{\delta 2}H$ 7.23; $C^{\epsilon 1}H$ 8.56
V21	8.98	3.37	1.63	$C^{\gamma}H_3$ 0.28, 0.25	N52	8.44	4.64	2.79, 2.67	
C22	8.34	5.10	3.10, 2.87		D53	8.77	4.65	3.18, 2.76	
G23	9.13	3.99, 3.80			G54	8.49	4.30, 4.19		
Q24	8.45	4.01	1.98, 1.98	$C^{\gamma}H$ 2.40, 2.40	D55	8.48	4.69	2.76, 2.67	
G25	8.65	4.19, 3.59			F56	8.08	4.51	2.79, 2.68	$C^{\delta}H$ 7.16; $C^{\epsilon}H$ 7.31; $C^{\zeta}H$ 7.20
N26	7.95	5.46	2.70, 2.60		E57	8.08	4.27	1.99, 1.99	$C^{\gamma}H$ 2.30, 2.30
K27	9.20	4.40	1.19, 1.19	$C^{\gamma}H$ 0.94, 0.94; $C^{\delta}H$ 1.38, 1.29	E58	8.16	4.30	2.01, 1.90	$C^{\gamma}H$ 2.37, 2.37
					I59	8.05	4.41	1.82	$C^{\gamma}H$ 1.42, 1.08; $C^{\gamma}H_3$ 0.88; $C^{\delta}H_3$ 0.77
				$C^{\epsilon}H$ 2.76, 2.62; $N^{\zeta}H$ 7.58	P60		4.32	2.23, 1.80	$C^{\gamma}H$ 1.97, 1.91; $C^{\delta}H$ 3.81, 3.60
C28	9.00	5.34	2.91, 2.79		E61	8.25	4.18	1.98, 1.90	$C^{\gamma}H$ 2.41, 2.41
I29	9.78	4.25	2.01	$C^{\gamma}H$ 1.45, 1.33; $C^{\gamma}H_3$ 0.80; $C^{\delta}H_3$ 0.67	E62	8.20	4.22	1.87, 1.87	$C^{\gamma}H$ 2.33, 2.25
					Y63	8.07	4.63	3.16, 2.94	$C^{\delta}H$ 7.19; $C^{\epsilon}H$ 7.33
L30	8.37	4.13	1.50, 1.50	$C^{\gamma}H$ 1.38; $C^{\delta}H_3$ 0.53, 0.53	L64	7.99	4.32	1.58, 1.58	$C^{\gamma}H$ 1.51; $C^{\delta}H_3$ 0.83, 0.79
G31	8.93	3.98, 3.48			Q65	8.12	4.27	2.11, 1.91	$C^{\gamma}H$ 2.30, 2.30
S32	8.09	4.62	3.75, 3.75						

NH–aliphatic, and $C^{\alpha}H$–$C^{\alpha}H$ NOE connectivities are shown in Figures 3–5, respectively.

A summary of the short-range ($|i-j| \leq 5$) NOEs involving the NH, $C^{\alpha}H$, and $C^{\beta}H$ protons as well as the $C^{\delta}H$ protons of proline is shown in Figure 6, and the resonance assignments are listed in Table I. In addition, Figure 6 provides a summary of the slowly exchanging (>24 h) NH protons and of the $^3J_{HN\alpha}$ coupling constants measured from the pure phase absorption ω_1-scaled DQF-COSY spectrum in H_2O.

The regular secondary structure elements present in hirudin can be identified from characteristic patterns of short-range NOEs (Wüthrich et al., 1984; Williamson et al., 1984; Wagner et al., 1986). There is no evidence for the presence of any helical elements characterized by a stretch of NH(i)–NH(i + 1), $C^{\alpha}H(i)$–NH(i + 3), and $C^{\alpha}H(i)$–$C^{\beta}H(i+3)$ NOEs and apparent values of $^3J_{HN\alpha}$ <5 Hz indicative of ϕ backbone torsion angles in the range −15 to −90° (Pardi et al., 1984). There are four β-strands extending from residues 15 to 16 (I), 21 to 22 (I′), 26 to 31 (II), and 36 to 42 (II′), characterized by a stretch of strong $C^{\alpha}H(i)$–NH(i + 1) NOEs and apparent values of $^3J_{HN\alpha}$ >8 Hz indicative of ϕ backbone torsion angles in the range −80 to −180° (Pardi et al., 1984). These four strands are arranged into two antiparallel β-sheets, comprising strands I and I′ and strands II and II′, characterized by a set of interstrand NH–NH, NH–$C^{\alpha}H$, and $C^{\alpha}H$–$C^{\alpha}H$ NOEs illustrated in Figure 7. Note that β-strand I has a β-bulge (Richardson, 1981) at residue 16 and that β-sheet II is distorted as evidenced by weak NH(i)–NH(i + 1) NOEs between residues 28 and 29, residues 29 and 30, residues 31 and 32, and residues 40 and 41. The two turns connecting β-strands

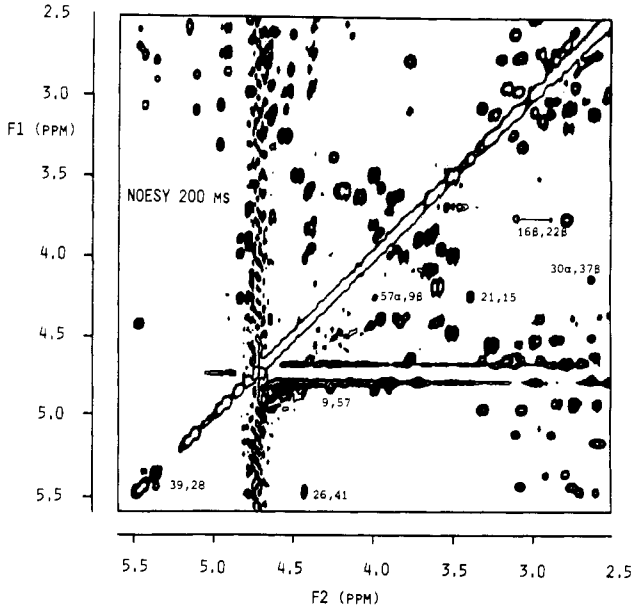

FIGURE 5: $C^{\alpha}H$(F1-axis)–$C^{\alpha}H$(F2-axis) region of the 200-ms NOESY spectrum of hirudin in D_2O. Long-range $C^{\alpha}H$–$C^{\alpha}H$ connectivities are indicated. Also indicated are the long-range $C^{\alpha}H$–$C^{\beta}H$ and $C^{\beta}H$–$C^{\beta}H$ NOEs present in this region of the spectrum. The spectrum is unsymmetrized.

I and I′ (residues 17–20) and β-strands II and II′ (residues 32–35) are classical β-turns. β-Strands I′ and II are also connected by a turn comprising residues 23–25. In addition, the two β-sheets are connected to each other by means of two

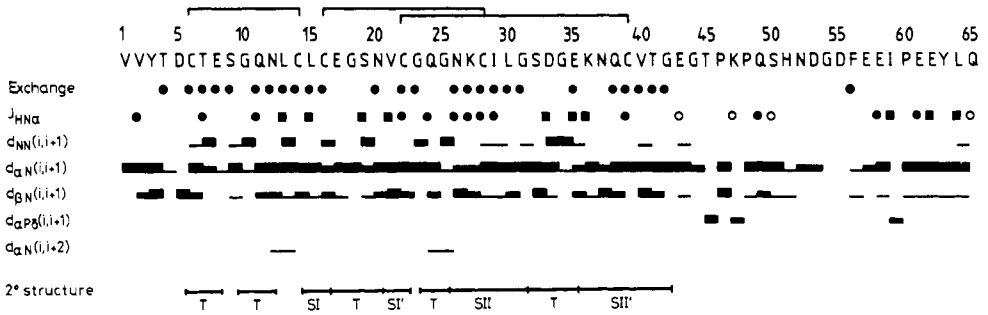

FIGURE 6: Sequence of hirudin together with a summary of the observed short-range NOEs involving the NH, $C^{\alpha}H$, and $C^{\beta}H$ protons as well as the $C^{\delta}H$ protons of the proline residues. The NOEs are classified into strong, medium, and weak by the thickness of the line. NH protons that are still present after 24 h of dissolving the protein in D_2O are indicated by closed circles (●). Apparent values of $^3J_{HN\alpha} > 10$ Hz, $8 < {}^3J_{HN\alpha} < 10$ Hz, and $^3J_{HN\alpha} < 6$ Hz as measured from the ω_1-scaled DQF-COSY spectrum in H_2O are indicated by the symbols ●, ■, and ○, respectively. The location of the disulfide bridges is indicated above the sequence.

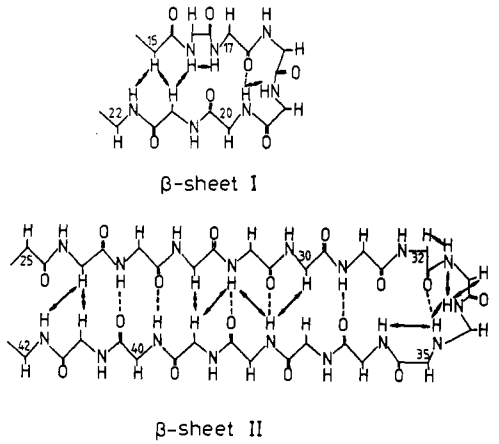

FIGURE 7: Diagrammatic representation of the two β-sheets of hirudin. The interstrand backbone NOEs as well as the short-range NH-(i)–NH(i + 1) and $C^{\alpha}H(i)$–NH(i + 1) NOEs in the two turns are indicated by arrows. Note the β-bulge in β-sheet I at residue 16. Backbone hydrogen bonds consistent with the NOE data and the NH exchange data (see Figure 6) are shown as dashed lines.

disulfide bridges between Cys-16 (strand I) and Cys-28 (strand II) and between Cys-22 (strand I′) and Cys-39 (strand II′). Associated with the two disulfide bridges are NOEs between the $C^{\beta}H$ protons of residues 16 and 28 and residues 22 and 39. Two other turns could be identified, comprising residues 6–8 and 10–12 that form a loop with the disulfide bridge between Cys-6 and Cys-14 at its base. These two turns as well as the turn from residue 23 to residue 25 could not be classified further on the basis of the present data.

The segments extending from residues 1 to 5, residues 13 to 14, and residues 42 to 65 form irregular strands. The polypeptide chain extending from residues 1 to 9 lies in close proximity to β-strands I′ and II as evidenced by the observation of NOEs from Tyr-3 to Leu-13, Cys-14, and Leu-15, from Thr-4 to Leu-15, from Glu-8 to Gln-24, Gly-25, and Asn-26, and from Ser-9 to Leu-30. The polypeptide chain extending from residue 43 to residue 65 forms a loop that folds back on the rest of the protein, and parts of this chain are in close proximity to residues 1–10; this is based on the observation of NOEs between Phe-56 and Thr-7 and between Gln-57 and Ser-9 and to β-strand II since an NOE between Phe-56 and Cys-28 is observed.

With the present data in hand, we are now in the process of assigning all long-range NOEs in order to determine the tertiary structure of hirudin using a combination of distance geometry (Havel & Wüthrich, 1985) and restrained molecular dynamics calculations (Clore et al., 1985, 1986a,b; Kaptein et al., 1985; Brünger et al., 1986).

ACKNOWLEDGMENTS

We thank Dr. R. Maschler and Prof. E. Fink (Plantorgan Werk AG) and Dr. D. Tripier (Hoechst) for the gift of hirudin.

Registry No. Hirudin, 8001-27-2.

REFERENCES

Bagdy, D., Barabas, E., Graf, L., Ellebaek, T., & Magnusson, S. (1976) *Methods Enzymol. 45*, 669–678.

Bax, A., & Davis, D. G. (1985) *J. Magn. Reson. 65*, 355–366.

Bergmann, C., Dodt, J., Kohler, S., Fink, E., & Gassen, H. G. (1986) *Biol. Chem. Hoppe-Seyler 367*, 731–740.

Braun, W., & Go, N. (1985) *J. Mol. Biol. 186*, 611–626.

Brown, L. R. (1984) *J. Magn. Reson. 57*, 513–518.

Brünger, A. T., Clore, G. M., Gronenborn, A. M., & Karplus, M. (1986) *Proc. Natl. Acad. Sci. U.S.A. 83*, 3801–3805.

Clore, G. M., Gronenborn, A. M., Brünger, A. T., & Karplus, M. (1985) *J. Mol. Biol. 186*, 435–455.

Clore, G. M., Brünger, A. T., Karplus, M., & Gronenborn, A. M. (1986a) *J. Mol. Biol. 191*, 523–551.

Clore, G. M., Nilges, M., Sukumaran, D. K., Brünger, A. T., Karplus, M., & Gronenborn, A. M. (1986b) *EMBO J. 5*, 2729–2735.

Clore, G. M., Martin, S. R., & Gronenborn, A. M. (1986c) *J. Mol. Biol. 191*, 553–561.

Dodt, J., Müller, H. P., Seemuller, U., & Chang, J. Y. (1984) *FEBS Lett. 165*, 180–184.

Dodt, J., Seemuller, U., Maschler, R., & Fritz, H. (1985) *Biol. Chem. Hoppe-Seyler 366*, 379–385.

Dodt, J., Machleidt, W., Seemuller, U., Maschler, R., & Fritz, H. (1986) *Biol. Chem. Hoppe-Seyler 367*, 803–811.

Harvey, R. P., Degryse, E., Stefani, L., Schamber, F., Cazenave, J. P., Courtney, M., Tolstoshev, P., & Lecocq, J. P. (1986) *Proc. Natl. Acad. Sci. U.S.A. 83*, 1084–1088.

Havel, T. F., & Wüthrich, K. (1985) *J. Mol. Biol. 182*, 281–294.

Haycraft, J. B. (1884) *Proc. R. Soc. London, B 36*, 478–487.

Ishikawa, A., Hafter, R., Seemuller, U., Gohel, J. M., & Graef, M. (1980) *Thromb. Res. 19*, 351–358.

Jeener, J., Meier, B. H., Bachmann, P., & Ernst, R. R. (1979) *J. Chem. Phys. 71*, 4546–4553.

Kaptein, R., Zuiderweg, E. R. P., Scheek, R. M., Boelens, R., & van Gunsteren, W. F. (1985) *J. Mol. Biol. 182*, 179–182.

Kline, A. D., & Wüthrich, K. (1985) *J. Mol. Biol. 185*, 503–507.

Kloss, T., & Mittman, U. (1982) *Langenbecks Arch. Chir. 358*, 548.

Magnusson, S. (1972) *Enzymes (3rd Ed.) 3*, 277–321.

Marion, D., & Wüthrich, K. (1983) *Biochem. Biophys. Res. Commun. 113*, 967–974.

Markwardt, F. (1970) *Methods Enzymol. 19*, 924-932.
Markwardt, F. (1985) *Biomed. Biochim. Acta 44*, 1007-1013.
Markwardt, F., Hauptmann, J., Nowak, G., Klessen, C., & Walsmann, P. (1982) *Thromb. Haemostasis 47*, 226-229.
Noggle, J., & Schirmer, R. E. (1971) *The Nuclear Overhauser Effect: Chemical Applications*, Academic, New York.
Nowak, G., & Markwardt, F. (1980) *Exp. Pathol. 18*, 438-443.
Otting, G., Widmer, H., Wagner, G., & Wüthrich, K. (1986) *J. Magn. Reson. 66*, 187-193.
Pardi, A., Billeter, M., & Wüthrich, K. (1984) *J. Mol. Biol. 180*, 741-751.
Plateau, P., & Gueron, M. (1982) *J. Am. Chem. Soc. 104*, 7310-7311.
Rance, M., Sorensen, O. W., Bodenhausen, G., Wagner, G., Ernst, R. R., & Wüthrich, K. (1983) *Biochem. Biophys. Res. Commun. 117*, 479-485.
Redfield, A. G., & Kuntz, S. D. (1975) *J. Magn. Reson. 19*, 250-254.
Richardson, J. S. (1981) *Adv. Protein Chem. 34*, 167-339.
Stone, S. R., & Hosteenge, J. (1986) *Biochemistry 25*, 4622-4628.
Strop, P., Wider, G., & Wüthrich, K. (1983) *J. Mol. Biol. 166*, 641-667.
Wagner, G., & Wüthrich, K. (1982) *J. Mol. Biol. 160*, 343-361.
Wagner, G., Neuhaus, P., Worgotter, E., Vasak, M., Kagi, J. H. R., & Wüthrich, K. (1986) *J. Mol. Biol. 187*, 131-135.
Walsmann, P., & Markwardt, F. (1981) *Pharmazie 36*, 653-660.
Wider, G., Macura, S., Kumar, A., Ernst, R. R., & Wüthrich, K. (1984) *J. Magn. Reson. 56*, 207-234.
Williamson, M. P., Marion, D., & Wüthrich, K. (1984) *J. Mol. Biol. 173*, 341-359.
Wüthrich, K., Wider, G., Wagner, G., & Braun, W. (1982) *J. Mol. Biol. 155*, 311-319.
Wüthrich, K., Billeter, M., & Braun, W. (1984) *J. Mol. Biol. 180*, 715-740.
Zarbock, J., Clore, G. M., & Gronenborn, A. M. (1986) *Proc. Natl. Acad. Sci. U.S.A. 83*, 7628-7632.
Zuiderweg, E. R. P., Kaptein, R., & Wüthrich, K. (1983) *Eur. J. Biochem. 127*, 279-292.

Functional Role of Proteolytic Cleavage at Arginine-275 of Human Tissue Plasminogen Activator As Assessed by Site-Directed Mutagenesis

Keri M. Tate, Deborah L. Higgins, William E. Holmes, Marjorie E. Winkler, Herbert L. Heyneker, and Gordon A. Vehar*

Department of Molecular Biology and Biochemistry, Genentech, Inc., South San Francisco, California 94080

Received October 3, 1986; Revised Manuscript Received November 17, 1986

ABSTRACT: Activation of the zymogen form of a serine protease is associated with a conformational change that follows proteolysis at a specific site. Tissue-type plasminogen activator (t-PA) is homologous to mammalian serine proteases and contains an apparent activation cleavage site at arginine-275. To clarify the functional consequences of cleavage at arginine-275 of t-PA, site-specific mutagenesis was performed to convert arginine-275 to a glutamic acid. The mutant enzyme (designated Arg-275 → Glu t-PA) could be converted to the two-chain form by *Staphylococcus aureus* V8 protease but not by plasmin. The one-chain form was 8 times less active against the tripeptide substrate H-D-isoleucyl-L-prolyl-L-arginine-*p*-nitroanilide (S-2288), and the ability of the enzyme to activate plasminogen in the absence of fibrinogen was reduced 20-50 times compared to the two-chain form. In contrast, one-chain Arg-275 → Glu t-PA has equal activity to the two-chain form when assayed in the presence of physiological levels of fibrinogen and plasminogen. Fibrin bound significantly more of the one-chain form of t-PA than the two-chain form for both the wild-type and mutated enzymes. One- and two-chain forms of the wild-type and mutated plasminogen activators slowly formed complexes with plasma protease inhibitors, although the one-chain forms showed decreased complex formation with α_2-macroglobulin. The one-chain form of t-PA therefore is fully functional under physiologic conditions and has an increased fibrin binding compared to the two-chain form.

The serine proteases comprise a family of enzymes that function in a wide variety of physiological processes (Reich et al., 1975). These enzymes are initially synthesized as inactive precursors that have slightly different conformations than their active forms (Stroud et al., 1975). The mechanism of activation of these zymogens occurs through limited proteolysis at a specific site (Neurath, 1975). This cleavage (at position 15 of the chymotrypsin numbering system) permits the new, positively charged α-amino group of residue 16 to form an ion pair with the polypeptide backbone at Asp-194 (Matthews et al., 1967; Sigler et al., 1968). Correlated with the formation of this ion pair are conformational changes (Neurath et al., 1956; Freer et al., 1970) that have been reported to increase the overall reaction rates of trypsin and chymotrypsin by factors of up to 10^7 (Neurath, 1975).

Human tissue plasminogen activator (t-PA)[1] is a key component of the group of proteins involved with fibrin dissolution (Verstraete & Collen, 1986). The carboxy-terminal 252 amino acids of this 527 amino acid glycoprotein share considerable homology with other serine proteases (Pennica et al., 1983;

[1] Abbreviations: t-PA, tissue-type plasminogen activator; KIU, Kallikrein Inactivator Units; Tris-HCl, tris(hydroxymethyl)aminomethane hydrochloride; SDS, sodium dodecyl sulfate; DTT, dithiothreitol.

0006-2960/87/0426-0338$01.50/0